

669

Appendix

670 A. Implementation Details

671 We mostly focus on longer videos because better frame se-
 672 lection plays a bigger role in longer, more complex videos,
 673 whereas shorter ones intuitively work well with uniform
 674 sampling due to their lower information content and com-
 675 plexity.

676 We ensured that the resulting sequence length of a set of
 677 visual and textual tokens did not exceed the maximum se-
 678 quence length for this LLM. When evaluating models using
 679 MaxInfo, we limited the number of selected frames so that
 680 they did not exceed the maximum allowed for the context of
 681 the estimated VLLM. For the evaluation on all benchmarks,
 682 we have set the generation temperature to 0.

683 For the general multiple-choice question-answering
 684 evaluation, we follow the official guidelines to construct the
 685 instructions using the provided questions and options. We
 686 added a prompt to the question and options like "*Respond*
 687 with only the letter (A, B, C, or D) of the correct option." for
 688 LongVideoBench [40], Video-MME [11], MLVU [53] and
 689 MVBench [20] or "*Answer with the option's letter from the*
 690 *given choices directly and only give the best option.*" for
 691 EgoSchema [23]. We follow the original benchmarks setup
 692 to calculate the final scores, and we also align our evaluation
 693 protocols with other evaluation toolkits, such as lmms-eval
 694 [49].

695 To ensure the reproducibility of our results, we have in-
 696 cluded the main hyperparameters used for all benchmarks
 697 and estimated models in the results tables, such as tolerance
 698 and rank for the MaxInfo algorithm, the number of sampled
 699 frames, and the number of initial frames (before MaxInfo).

700 B. Additional Experiments and Details

701 To further assess the impact of MaxInfo, we evaluate its
 702 performance with an additional set of models [37], [46] on
 703 the LongVideoBench and Video-MME benchmarks.

704 B.1. Applying MaxInfo to recent models

705 The results in Table 6 show that MaxInfo consistently im-
 706 proves model performance across both benchmarks, sug-
 707 gesting that precise frame selection is particularly important
 708 for long-video tasks.

709 B.2. Performance Analysis: MaxInfo vs. Uniform 710 Sampling

711 To better understand the strengths and trade-offs of Max-
 712 Info, we analyzed per-task accuracy across multiple bench-
 713 marks. Our results, as shown in Figure 6, indicate that Max-
 714 Info performs superiorly in high information density tasks
 715 such as counting, summarizing and spatial reasoning, while

Table 6. Adaptation of MaxInfo to current new long video under-
 standing models

Model	Size	Frame Interval	Avg. frames	LongVideoBench
MiniCPM [46]	9B	128	128	56.17
+ MaxInfo	9B	[8, 82]	56	59.61
△				+3.44
InternVL3.5 [37]	1B	16	16	47.7
+ MaxInfo	1B	[1, 16]	16	49.0
△				+1.3
InternVL3.5 [37]	8B	16	16	57.4
+ MaxInfo	8B	[1, 16]	16	59.0
△				+1.6
InternVL3.5 [37]	38B	16	16	60
+ MaxInfo	38B	[1, 16]	16	61.6
△				+1.6

uniform sampling has a slight advantage in tasks that rely
 716 on temporal continuity, reflecting the key trade-off between
 717 information maximization and temporal consistency.
 718

719 B.3. Comparison with CLIP baseline

720 As shown in Table 7, we compare the experimental re-
 721 sults of two keyframe extraction strategies based on the
 722 QwenVL2-2B model on the LongVideoBench benchmark:
 723 the **CLIP-Based** thresholding method and the **MaxInfo**
 724 module method. Both methods extract the same number
 725 of frames in the initial phase, so the encoding time is kept
 726 the same, where the similarity threshold of the CLIP-Based
 727 method is set to 0.5. The results show that the MaxInfo
 728 module outperforms the CLIP-Based method in terms of the
 729 overall performance in keyframe selection.

Table 7. Performance comparison on LVbench.

Model	Method	Accuracy
QwenVL2-2B	CLIP-Based	44.3
QwenVL2-2B	CLIP-Based + MaxInfo	44.5
QwenVL2-2B	MaxInfo + CLIP-Based	43.8
QwenVL2-2B	MaxInfo	48.8

730 In addition, we also explored combining the CLIP-Based
 731 method with MaxInfo module. The experiments show that
 732 MaxInfo is able to improve the overall information qual-
 733 ity of the input sequences, and its information maximiza-
 734 tion strategy plays a key role in frame selection, which fur-
 735 ther enhances the performance of the model. CLIP-Based
 736 loses a lot of semantic information, which can lead to per-
 737 formance degradation of the model.

738 In order to further evaluate whether MaxInfo will lose
 739 the key frames related to the problem, we compare Max-
 740 Info with the Uniform Sampling method under the CLIP
 741 Score metric. The experimental results shown in Table 8
 742 that MaxInfo does not miss the frames related to the se-
 743 mantics of the problem, and is able to retain the semantic
 744 relevance effectively.

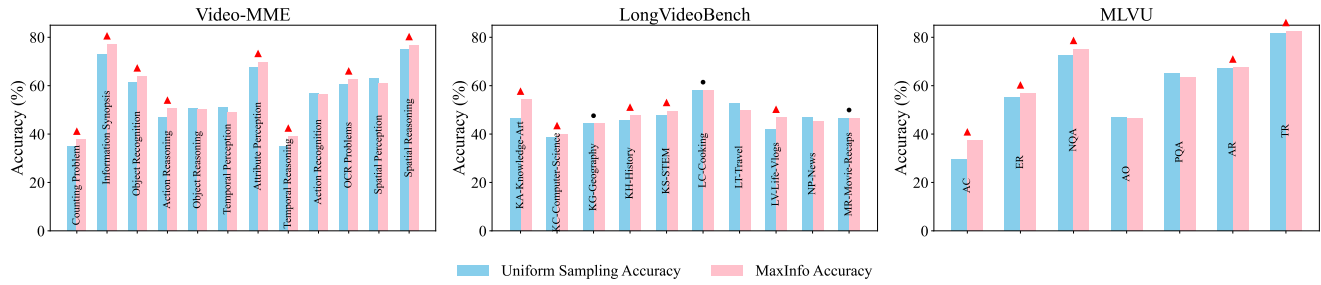


Figure 6. Accuracy comparison between Uniform Sampling and MaxInfo across three benchmarks.

Table 8. CLIP score comparison between uniform and MaxInfo sampling.

Sampling Method	CLIP-score
Uniform	0.37
MaxInfo	0.39

758
759

745

B.4. Qualitative comparison with uniform samplir

746

We randomly selected 50 video samples from LongVideoBench and calculated the cosine similarity between the frames selected by MaxInfo and the cosine similarity between the frames obtained by uniform sampling.

747

Figure 7 shows the distribution of cosine similarity for the same number of frames. It is clear that MaxInfo produces a more diverse distribution like a low similarity offset compared to uniform sampling, highlighting its ability to capture more diverse visual content.

748

749

750

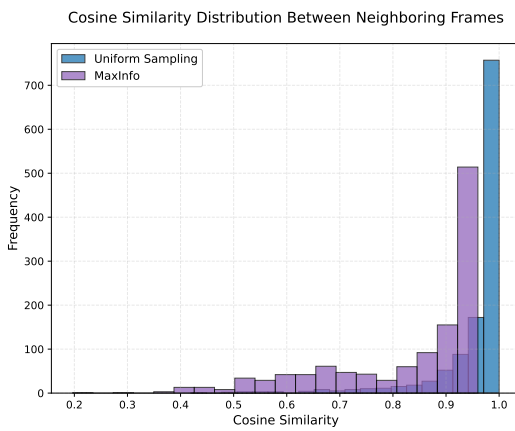
751

752

753

754

755

Figure 7. Similarity distribution between neighbouring frames ($frame_i$ and $frame_{i+1}$).

756

As shown in Figure 8, we plotted 200 sampled data points to improve visual clarity. The results show that our

MaxInfo module exhibits higher diversity in frame selection compared to uniform sampling.

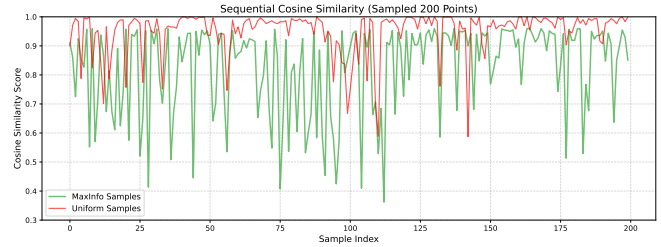


Figure 8. CLIP similarity between neighboring frames selected by MaxInfo module.

B.5. Computational Efficiency: Time and Memory Consumption

760
761

When processing long videos, the LLM is the most resource-intensive component of VLLMs due to its parameter count and the quadratic complexity of attention with respect to input length. Since most of the context is occupied by visual tokens from frames, our MaxInfo method reduces this load by selecting keyframes. Importantly, MaxInfo requires minimal and constant memory and preprocessing time, independent of LLM size, and remains significantly lighter than uniformly sampling all frames.

762
763
764
765
766
767
768
769
770

Time Complexity. To evaluate the latency overhead of MaxInfo in practice, we measured its runtime with the Qwen2-VL model. As shown in Table 9, the runtime of MaxInfo is almost negligible compared to the inference time of the VLLM itself, confirming that MaxInfo is a lightweight and efficient frame selection mechanism. The initial VLLM time means the inference time of the 512 frames of information directly into the Qwen2-VL model. The frame count selected by MaxInfo Block is adaptive to the information content of the input. For near-static videos (low information density), MaxInfo drastically reduces the number of processed frames. Consequently, VLLMs +

771
772
773
774
775
776
777
778
779
780
781
782

783 MaxInfo Block may achieve lower time compared to the
 784 initial VLLMs + MaxInfo Block configuration. The times
 785 reported in the table represent an upper bound; in prac-
 786 tice, the reduced number of frames can lead to several-fold
 787 speedups on certain tasks. All experiments were conducted
 788 on an A100 GPU.

Table 9. Runtime of different pipeline components, based on Qwen2-VL. Frame size = 512 (UP is Upper Bound).

Model Size	CLIP (s)	MaxVol (s)	VLLMs (s)	VLLMs + MaxInfo (UP)
2B	0.296	0.0109	2.979	≤ 3.285
7B	0.296	0.0109	5.372	≤ 5.679
72B	0.296	0.0109	30.737	≤ 31.044

789 We also analyzed the running time of the MaxVol algo-
 790 rithm alone, including its chunk-based variant, under differ-
 791 ent initial numbers of frames, as shown in Table 10. The
 792 experimental results show that the running time of MaxVol
 793 remains low across settings, with minimal impact on the
 794 overall inference efficiency.

Table 10. MaxVol algorithm runtime (excluding image encoding time) for different input sizes.

Method	Input Size	MaxVol Time (s)
MaxInfo	128	0.0044
MaxInfo	256	0.0053
MaxInfo	512	0.0109
Chunks-Based MaxInfo	32 × 32	0.0375

795 Then we estimated CUDA inference time across differ-
 796 ent VLLM sizes which is shown in Figure 9. The overhead
 797 of MaxInfo remains small and nearly constant, while the
 798 overall inference time grows with model size, demon-
 799 strating that MaxInfo adds minimal cost compared to the savings
 800 from reduced visual tokens. For small models (up to 8B para-
 801 meters), the relative benefit is limited since inference cost
 802 is low. However, for larger models (26B–76B), MaxInfo
 803 provides clear efficiency gains by substantially reducing the
 804 number of visual tokens, making its impact especially pro-
 805 nounced for long-video tasks where input length dominates
 806 computational cost.

807 **Memory Consumption.** Secondly, we precisely eval-
 808 uated memory consumption of our approach. As shown in
 809 Figure 10, MaxInfo’s CUDA memory usage remains con-
 810 stant for a fixed number of initial frames and grows much
 811 more slowly than uniform sampling as LLM size increases.

812 In summary, our analysis of time and memory efficiency
 813 shows that MaxInfo introduces only negligible overhead
 814 while substantially reducing the computational burden of
 815 processing long videos. Its constant preprocessing cost and
 816 slower growth in memory usage make MaxInfo particularly
 817 advantageous for large-scale VLLMs, with the benefits be-

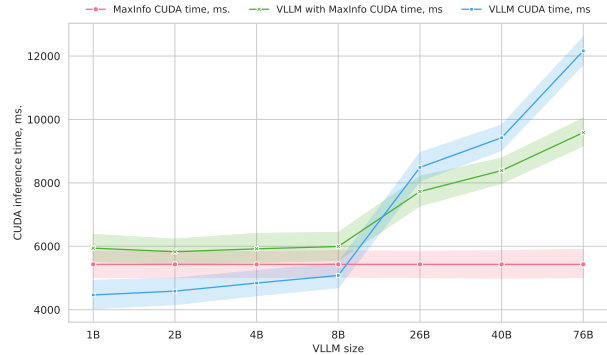


Figure 9. CUDA inference time across different VLLM sizes. The preprocessing cost of MaxInfo remains small and nearly constant, while overall inference time increases with model size.

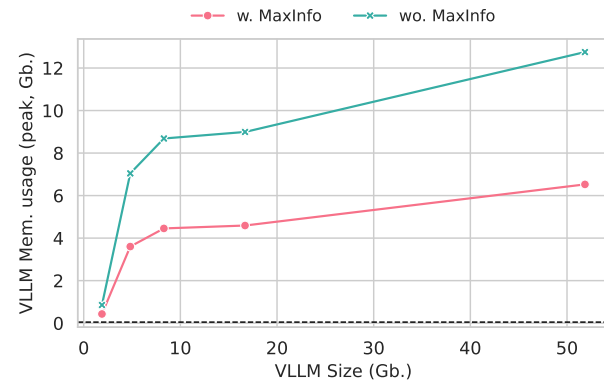


Figure 10. The comparison for memory performance on the GPU for InternVL2 models with and without MaxInfo module. The dashed line shows the CUDA memory requirements for MaxInfo.

coming most pronounced for models exceeding 10B parameters.

C. Theoretical Justification

Definition 1. *Definition of the maximum volume of the video frame feature matrix.*

We consider a matrix $Q \in \mathbb{C}^{N \times r}$, where each row represents the CLIP or SigLIP etc. feature of a video frame, ordered sequentially in time, where N denotes the number of frames and r denotes the dimension of the feature.

We aim to identify a submatrix $\hat{Q} \in \mathbb{C}^{K \times r}$ of the original matrix S , such that \hat{S} closely approximates S in terms of matrix volume, thereby preserving its essential structural information.

To obtain the submatrix \hat{Q} , we introduce a coefficient matrix C based on the minimum-norm linear combination as Equation 10

$$\tilde{C}\hat{Q} = \tilde{Q} \quad (10)$$

818
819

820

821
822

823
824
825
826

827
828
829
830

831
832
833
834

835 Here, \tilde{Q} denotes a set of sample rows selected from the original matrix Q for reconstruction. By solving for \tilde{C} , we can
 836 approximate the reconstruction of \tilde{Q} using only the representative rows in \tilde{Q} . In addition, it is shown that the selected
 837 K rows are the most representative of the video frame information.
 838

839 **Solving.** The submatrix $\hat{Q} \in \mathbb{C}^{K \times r}$ provides an approximation of the original matrix $Q \in \mathbb{C}^{N \times r}$ within a tolerance
 840 τ .

841 We start with an initial submatrix $\hat{Q} \in \mathbb{C}^{M \times r}$ and add
 842 a row $Q_i \in \mathbb{C}^{1 \times r}$ to each iteration to bring the expanded
 843 submatrix up to speed in the sense of volume. The updating
 844 process can be expressed as follows Equation 11 and the
 845 volume of the updated matrix can be defined as Equation 12

$$849 \hat{Q} \leftarrow \begin{bmatrix} \hat{Q} \\ Q_i \end{bmatrix} \quad (11)$$

$$850 \text{Vol}(\hat{Q})_{\text{new}} = \text{Vol}(\hat{Q})_{\text{old}} \cdot \sqrt{1 + \|\tilde{C}_i\|_2^2} \quad (12)$$

851 where Q_i is the row selected from the original matrix $Q \in$
 852 $\mathbb{C}^{N \times r}$ that currently boosts the volume of the submatrix the
 853 most. Repeat this process iteratively until the conditional
 854 Equation 13 is satisfied or the target number of K rows is
 855 reached.

$$856 \|\tilde{C}_i\|_2 \leq \tau \quad (13)$$

857 **Proof of maximum information entropy.** To justify our
 858 approach, we use differential entropy as an information
 859 measure. Suppose our normalized frame embeddings form
 860 a matrix S . The differential entropy of a uniform distribution
 861 over the convex hull $\mathcal{C}(S)$ is given by the following
 862 Equation 14.

$$863 H_{\max}(S) = \ln(\text{Vol}(\mathcal{C}(S))) \quad (14)$$

864 where $\text{Vol}(\mathcal{C}(S))$ is the volume of the convex hull formed by
 865 selected embeddings. Classical results show the following
 866 Equation 15.

$$867 \text{Vol}(\mathcal{C}(S)) = \kappa \sqrt{\det(S^\top S)} \quad (15)$$

868 for some constant $\kappa > 0$. Thus we get Equation 16

$$869 H_{\max}(S) = \ln V(S) + \text{constant} \quad (16)$$

870 where $V(S) = \sqrt{\det(S^\top S)}$. Since MaxVol maximizes
 871 $V(S)$, it maximizes the upper bound on differential entropy,
 872 ensuring that selected frames are more informative.

873 In summary, we can theoretically select the most rep-
 874 resentative frame information. The feature matrices corre-
 875 sponding to the selected frames have good linear indepen-
 876 dence under the constraint of the tolerance parameter τ , thus
 877 constituting an approximately optimal subset of the repre-
 878 sentation. This process achieves our goal of **information**
 879 **maximization**, i.e. preserving the most critical structural
 880 information while compressing redundancy.

D. Societal Impacts

882

This work introduces a training-free framework for improving frame sampling in Vision-Language Large Models (VLLMs), enhancing video understanding tasks. Such advancements have important implications for applications in education, accessibility, and public safety.

883

However, improved video analysis capabilities may also raise ethical concerns, including potential misuse in surveillance, privacy violations, or biases affecting different communities. Ensuring responsible deployment with fairness and transparency is essential to mitigate these risks.

884

In summary, while our approach provides significant benefits, its adoption should adhere to ethical principles to promote equitable and responsible use.

885

886

887

888

889

890

891

892

893

894

895